NASA TECHNICAL MEMORANDUM

NASA TM X-68071

NASA TM X-68071

EFFECT OF CONTACT ANGLE HYSTERESIS ON MOVING LIQUID FILM INTEGRITY

by F. F. Simon and Y. Y. Hsu
Lewis Research Center
Cleveland, Ohio

TECHNICAL PAPER proposed for presentation at
Seventy-third National Meeting of the
American Institute of Chemical Engineers
Minneapolis, Minnesota, August 27-30, 1972

EFFECT OF CONTACT ANGLE HYSTERESIS ON MOVING LIQUID FILM INTEGRITY

by F. F. Simon and Y. Y. Hsu

Lewis Research Center

E-6955

ABSTRACT

A study was made of the formation and breakdown of a water film moving over solid surfaces (teflon, lucite, stainless steel, and copper). The flow rate associated with film formation was found to be higher than the flow rate at which film breakdown occurred. The difference in the flow rates for film formation and film breakdown was attributed to contact angle hysteresis. Analysis and experiment, which are in good agreement, indicated that film formation and film breakdown are functions of the advancing and receding angles, respectively.

INTRODUCTION

Liquid-gas interfacial mass transfer or heat transfer is most efficient when the liquid medium has a large surface area to volume ratio. The need for a large surface area for a minimum volume is what determines the use of packed towers for scrubbing purposes in the recovery of chemicals and in the prevention of pollutant emission. A thin liquid film governs the heat transfer in one type of saline water evaporation and in the annular flow regime of two phase flow. Since the efficiency of the above transport processes requires that the liquid film be both very thin and stable, it is important to know the limiting flow rate conditions for realizing such a film. One limit is the flow rate per unit width required to

completely cover an originally unwetted surface without forming rivulets or dry spots. The other limit is the minimum flow rate on an initially wetted surface required to maintain a completely wetted surface. The first limiting flow rate is a wetting process for the formation of a complete liquid film and the second flow rate is a "dewetting" process for the breakdown of the liquid film. This paper will investigate the criteria for the onset of both wetting and dewetting processes. Specifically, this paper treats the case of a falling water film on surfaces of copper, teflon, lucite, and stainless steel rods. This range of surface materials permits an investigation wherein the wettability characteristics can be varied.

BACKGROUND

As a means of predicting the minimum flow rate, (i. e., the lowest flow rate that permits wetting of a surface) Hartley and Murgatroyd (ref. 1) proposed a force balance at the triple interface (vapor, liquid, and solid) of a liquid film. This was done for the case of a gravity motivated liquid film (falling film) and a shear motivated liquid film (annular flow). The motivation of the authors of ref. 1 was to find an expression for the minimum flow rate at which liquid film breakdown would occur at an originally wetted surface. In the model proposed by the authors of ref. 1, no distinction was made between a surface previously wetted and one which was about to undergo wetting. The analytical results of ref. 1 indicate that the minimum flow rate (or minimum film thickness) required for the wetting of a surface is a function of the fluid properties, the shear distribution and the static contact angle. For a falling liquid film, ref. 1 indicates that the minimum flow rate required for wetting is

$$\Gamma_{min} = 1.69\left(\frac{\mu\rho}{g}\right)^{1/5}\left[\gamma_{L\text{-}a}(1 - \cos\theta)\right]^{3/5} \qquad (1)$$

where θ is the static contact angle. The authors of ref. 1 could not prove the validity of equation (1) because they lacked sufficient information on the contact angle. A test of the Hartley and Murgatroyd analysis was made in ref. 2 for a shear motivated climbing film. This was done by producing a dry patch and noting if the dry area would be re-wetted. Measurement of the static contact angle was made for input to the theoretical calculation of the minimum flow rate. The calculated flow rate over-predicted the experimental value for re-wetting. The authors of ref. 2 reported that the static contact angle may not be the appropriate angle for the Hartley and Murgatroyd analysis since an advancing triple interface should produce a larger angle than a static value. However, since a larger angle would make the theory depart further from the experimental values, the authors suggested that an additional force was required in the analysis of Hartley and Murgatroyd. To take this discrepancy into account, Murgatroyd (ref. 3) proposed the addition of shear and form forces in the analysis of ref. 2. On the other hand, results using the Hartley-Murgatroyd analysis (eq. (1)) without the correction of ref. 3 were reported in ref. 4 for liquid film breakdown of a falling liquid film under mass transfer conditions. The experimental results of this reference show good agreement with equation (1). Therefore, the validity of equation (1) remains unclear.

One of the uses made of the Hartley-Murgatroyd analysis is to determine the stability of a dry patch (i. e., the persistence of dry patch) for

a heated or unheated surface. This purpose has already been mentioned above (ref. 2) and was further explored in refs. 5 and 6. Equation (1) indicates that there should be one unique response between dry patch stability and flow rate. Investigations of dry patch stability indicate that a dry patch is more stable over a larger flow range than indicated by equation (1). It was noted in refs. 6 and 7 that the value of the contact angle depended on whether a surface was being wetted or de-wetted, the contact angle being higher than the static value for the case of a triple interface advancing over an unwetted area and lower than the static value when the triple interface receded from a previously wetted area. This result is consistent with the well-known hysteresis of the contact angle. The authors found (ref. 8) that in the case of large amplitude, wavy film flow over a heated surface, the stability of a dry spot is a function of the wave profile. Such a wave profile permits the dewetting at the wave valley and a re-wetting of the dry spot as the wave crest moves by. Hartley and Murgatroyd's analysis (eq. (2)) was used for predicting the stability of such dry spots and it was found that a much larger contact angle than the static one was needed to properly correlate dry spot stability. Thompson and Murgatroyd (ref. 7) also noted that the presence of waves promoted wetting.

In summary, all the previous studies seem to indicate that for a falling film, several features stand out:

1. The flow rate required to wet an unwetted surface is greater than the flow rate for the initiation of a dry patch on a wetted surface.

2. The analytical model of Hartley and Murgatroyd does not predict either of the two flow rates mentioned previously.

3. For a wavy film, the wave valleys tend to initiate a dewetting process and the wave crests tend to rewet the dry spot formation.

What follows in this paper is an attempt to justify the basic analytical approach of Hartley and Murgatroyd and to extend this approach so that the analysis can comprehend both the wetting and de-wetting aspects of film flow by incorporating the concept of contact angle hysteresis. No attempt was made to include wavy film flow in the analysis.

NOMENCLATURE

A	area, cm^2
F	surface free energy, erg
f	wetting and de-wetting energy, erg/cm^2
g	gravitational acceleration, 980 cm/sec^2
P	pressure, N/m^2
u	velocity in x-component, cm/sec
W	work, erg
x	coordinate in flow direction
y	coordinate perpendicular to solid surface
z	coordinate normal to flow direction and parallel to surface
Γ	flow rate per unit length, g/cm-sec
γ	interfacial energy, erg/cm^2, or interfacial tension, dynes/cm
Δ	small increment
δ	film thickness, cm
θ	contact angle, deg

μ viscosity, g/cm-sec

ρ density, g/cm^3

Subscripts:

a advancing

d-w dewetting

f fluid

ℓ-a liquid-air

r receding

s-ℓ solid-liquid

s-a solid-air

w wetting

ANALYSIS

In this section the formation and breakdown of a gravity-motivated liquid film will be analyzed. The model which is being considered for the analysis is shown in fig. 1. This model was used in the force balance approach of Hartley and Murgatroyd (ref. 1) for the determination of the minimum flow rate as a function of the static contact angle. In this study, the consideration of an additional surface energy due to roughness, contamination, etc. makes it convenient to use an energy approach to the analysis. It is assumed that the falling liquid film is in laminar flow and that the waves on the film surface do not effect the wetting process.

Fig. 1 depicts the flow streamlines of a moving liquid film about an unwetted area. Streamline A-B is the key streamline to the analysis because the movement of point B determines whether the surface will be wetted or de-wetted. Point B will be displaced downstream (wetting)

when the liquid film flow increases sufficiently and displaced upstream (de-wetting) when there has been a decrease in the film flow.

The movement of point B will be in response to the imbalance of flow energy and surface energy existing in the vicinity of point B. The criterion for wetting and de-wetting will be determined from a flow and surface energy balance. At the start of the wetting or de-wetting process point B moves at infinitesimally slow velocity, thus B can be considered stationary at the threshold of transition and the velocity field $[u(y)]$ converts to a dynamic head P_d along B-C according to the following equation:

$$P_d = \frac{\rho}{2} [u(y)]^2 \tag{2}$$

When point B begins to show movement, the pressure field does a quantity of work given by

$$W_f = \left[\int_0^{\delta} P_d(y) dy \right] \Delta z \, \Delta x \tag{3}$$

Using the velocity distribution of a laminar falling film

$$u(y) = \frac{\rho g}{2\mu} (2y\delta - y^2) \tag{4}$$

and combining it with equations (2) and (3), the flow work is expressed as

$$W_f = \left[\frac{\rho^3 g^2}{8\mu^2} \int_0^{\delta} \left(2y\delta - y^2\right)^2 dy \right] \Delta z \, \Delta x \tag{5}$$

Equation (5) allows us to calculate the available flow work as a function of film thickness. The surface work involved in the wetting or dewetting process is obtained from the surface free energy change. The total surface free energy for a surface undergoing wetting is

$$F_w = \gamma_{s-l} A_{s-l} + \gamma_{s-a} A_{s-a} + \gamma_{l-a} A_{l-a} + f_w A_{s-l} \tag{6}$$

where f_w is the additional energy associated with the wetting process and which is likely related to such things as surface roughness and surface contamination. (An absorbed layer of liquid molecules can also be the cause of additional energy as shown in ref. 9.) The change of the surface free energy given by equation (6) results in wetting work.

$$W_w = \gamma_{s-l} \Delta A_{s-l} + \gamma_{s-a} \Delta A_{s-a} + \gamma_{l-a} \Delta A_{l-a} + f_w \Delta A_{s-l} \tag{7}$$

Since

$$\Delta A_{s-l} = \Delta A_{l-a}$$

$$\Delta A_{s-l} + \Delta A_{s-a} = 0$$

then

$$W_w = (\gamma_{s-l} + \gamma_{l-a} - \gamma_{s-a} + f_w)\Delta A_{s-l} \tag{8}$$

At this point we relate the energies of equation (8) to a measureable quantity, the contact angle. Since the surface energy per unit area is equivalent to a force per unit length acting over a unit displacement, the

energies of equation (8) can be treated as forces acting along the tangent at the triple interface (fig. 2). A vector balance is thus obtained which gives in the case of wetting

$$\gamma_{l\text{-}a} \cos \theta_a = - f_w + \gamma_{s\text{-}a} - \gamma_{s\text{-}l} \tag{9}$$

Eliminating the additional energy (f_w) in equation (9) gives the Young-Dupre equation for a static contact angle.

Substitution of equation (9) into equation (8) gives

$$W_w = (\gamma_{l\text{-}a} - \gamma_{l\text{-}a} \cos \theta_a)\Delta A_{s\text{-}l} \tag{10}$$

or since

$$\Delta A_{s\text{-}l} = \Delta z \, \Delta x$$

$$W_w = \gamma_{l\text{-}a}(1 - \cos \theta_a)\Delta z \, \Delta x \tag{11}$$

The work required for de-wetting follows the same approach as for the wetting process above except for the assumption that an initial dry area will spontaneously form on a surface which was initially all wetted. The authors' experimental experience indicates that in the case of a falling liquid film, there are sufficient disturbances at the liquid-air interface to permit a dry spot to form momentarily. Determination of the surface energy involved with the growth of such a dry spot (de-wetting) follows the approach given above for the wetting case.

The de-wetting work is determined from the free energy change.

$$W_{d\text{-}w} = \gamma_{s\text{-}l} \Delta A_{s\text{-}l} + \gamma_{s\text{-}a} \Delta A_{s\text{-}a} + \gamma_{l\text{-}a} \Delta A_{l\text{-}a} + f_{d\text{-}w} \Delta A_{s\text{-}a} \tag{12}$$

Following the procedure for the wetting case we obtain

$$W_{d-w} = (\gamma_{s-l} + \gamma_{l-a} - \gamma_{s-a} + f_{d-w})\Delta z\, \Delta x \tag{13}$$

For an interface which is moving from a previously wetted surface, the relevant contact angle is the receding contact angle which is related to the energies in the region of the triple interface.

$$\gamma_{l-a} \cos \theta_r = f_{d-w} + \gamma_{s-a} - \gamma_{s-l} \tag{14}$$

A combination of equations (3) and (14) results in

$$W_{d-w} = \gamma_{l-a}(1 - \cos \theta_r)\Delta z\, \Delta x \tag{15}$$

For determining the flow rates that separate a fully wetted surface condition and a partially wetted surface condition, the following conditions must hold:

$$W_f \geq W_w \qquad \text{for wetting an initially dry surface} \tag{16a}$$

$$W_f \leq W_{d-w} \qquad \text{for de-wetting an initially wet surface} \tag{16b}$$

Use is made of the above balance of flow and wetting work, equations (5), (11), and (15) and the flow equation

$$\Gamma = \frac{\rho^2 g \delta^3}{3\mu} \tag{17}$$

to obtain the theoretical equations for the flow rates at which there is a transition from an unwetted to a wetted condition and a wetted to a de-

wetted condition, respectively:

$$\Gamma_w = 1.69 \left(\frac{\mu\rho}{g}\right)^{1/5} \left[\gamma_{l\text{-}a}(1 - \cos\theta_a)\right]^{3/5} \tag{18a}$$

$$\Gamma_{d\text{-}w} = 1.69 \left(\frac{\mu\rho}{g}\right)^{1/5} \left[\gamma_{l\text{-}a}(1 - \cos\theta_r)\right]^{3/5} \tag{18b}$$

Both equations (18a) and (18b) can be expressed as a single equation:

$$\Gamma^* = 1.69 \left(\frac{\mu\rho}{g}\right)^{1/5} \left[\gamma_{l\text{-}a}(1 - \cos\theta^*)\right]^{3/5} \tag{19}$$

where

$$\Gamma^* = \Gamma_w, \qquad \theta^* = \theta_a \qquad \text{for wetting}$$

$$\Gamma^* = \Gamma_{d\text{-}w}, \qquad \theta^* = \theta_r \qquad \text{for de-wetting}$$

Equation (19) gives, for a specified fluid, the relationship between the wetting and de-wetting flow rates in terms of advancing and receding contact angles, respectively. The experimental phase of this study attempts to demonstrate the utility of these equations.

EXPERIMENTAL METHOD

The experimental phase is divided into two main parts. The first part describes the manner in which the experimental wetting and de-wetting flow rates of water on four surfaces were determined. The second part describes the measurement of the advancing and receding contact angles for water on the four test surfaces employed in the first part.

Wetting and De-wetting Flow Rates

The experimental system was designed for a continuous water film to be placed on the outside of vertical rods (fig. 3). The rod geometry obviates the problem of end effects in the film as would occur if the film were flowing in a channel. The rods were 1.27 cm in diameter and 60 cm long (wetted section). Surface energy variation of the solid surface was achieved by having rods of lucite, teflon, copper, and stainless steel. Fig. 3 shows the manner in which the rods were placed with respect to a reservoir. The liquid film was developed by flow from the reservoir through an annular slit (0.3 cm width) surrounding the rod. Glass wool was placed in the annular space so that a good entrance flow distribution could be achieved. To achieve uniform flow distribution along the length of the rod, adjustments were made in the vertical alignment of the rod until the water bob at the bottom of the rod was visually judged to be symmetrical.

The stainless steel and copper rods were polished with crocus cloth and levigated alumina. This procedure gave a surface sufficiently smooth to minimize roughness-wetting effects. Flow rates for the copper rod were determined immediately after polishing so as to avoid as much as possible effects due to oxidation of the copper. Prior to obtaining flow data, the rods were cleaned with detergent and rinsed with water. The wetting flow rate was determined by beginning with an unwetted surface and gradually increasing the water flow rate in small increments until incipience of complete wetting of the surface occurred. Once a stable liquid film covered the entire rod, a gradual lowering of

the flow rate in small increments was begun to obtain film breakdown or de-wetting. Immediately after the start of the de-wetting process, which began at the bottom of the rod, a large fraction of the surface quickly lost its covering of water. The flow rate corresponding to this condition was taken as the de-wetting flow rate. The above procedure of wetting and de-wetting was repeated several times to insure that the results were reproducible. Flow rates and water temperatures were measured at the exit position with a graduate cylinder, a stop watch and a mercury thermometer. The flow rates were measured over a period of about 30 sec. The flow rate per unit length Γ was determined by dividing the overall flow rate with rod circumference.

Advancing and Receding Contact Angles

To obtain the contact angles associated with wetting and de-wetting, water drops were placed on the rods used in the flow rate experiments (fig. 4). Cleaning and polishing of the rods was performed as in the flow rate experiments. Use of the same rods, with small drops, permits the approximate reproduction of the contour effect on the triple-interface as that in the falling film. The rods were caused to rotate about an axis perpendicular to the rod axis from their horizontal position until a condition of drop sliding was reached. Since the sliding drop causes wetting (in the front of the drop) and de-wetting (in the rear of the drop) of the surface, a knowledge of the contact angles associated with wetting (advancing contact angle) and de-wetting (receding contact angle) can be used as input to equations (18a) and (18b). Movies were taken of the drop as it deformed and then finally went sliding along the

surface. It was found necessary to keep the camera and rod on the same rotating plane (fig. 4) so that the camera would always see the same view of the triple interface. Measurements were made from the movie film for a determination of the contact angles associated with the advancing and receding triple interfaces of the drop. Since the contact angle varies with the velocity of the interface, the contact angles that corresponded with the beginning of motion of the triple interface, were taken as the appropriate angles for equation (19).

RESULTS AND DISCUSSION

In this section the result of this study will be presented and discussed first. Then the results of earlier works in the literature will be re-examined and re-interpreted with the hope that some of the apparent discrepancies between Hartley-Murgatroyd's analysis and the expermental data can be explained with the present model.

Present Results

Wetting and De-wetting Flow Rates. - The first event observed in the wetting of a rod was the appearance of a rivulet 1/2 cm or less in width. The manner in which such a rivulet spirals around the rod is shown in fig. 5(a). With increasing flow rate, the rivulet width increased and additional rivulets became evident (no more than three at one time in our experiments). The initial wetting process appeared to be governed by the laterial growth of rivulets. Such a process should govern the wetting of small diameter cylinders and wires. After the rivulets grew and joined together, the next condition encountered was a continuous liquid film at the top region of the rod and an unwetted region

on the remainder of the rod (fig. 5(b)). Once a flow rate was reached wherein the wetting front began to advance, it was only a matter of time (typically, less than a minute) before the entire surface became wetted. It is this second part of the wetting process that the analysis is directed to. Fig. 5(c) shows the fully wetted condition achieved at the wetting flow rate Γ_w. It is recalled that in the analysis, the effect of the film wave motion on the wetting process was not considered. In our experiments the wetting began at the top 1/3 of the rod. At this position there was insufficient length for waves to fully develop and impart their energy to the stagnant front of the triple interface.

Roughness was found to have an important role in the de-wetting process for surfaces of good wettability (low θ_r) such as copper and stainless steel. Initially, the copper rod was given a final polishing with crocus cloth. The roughness obtained from this procedure permitted a very thin layer of water to adhere to the copper rod after the water flow was stopped. This effect is equivalent to a zero value of the receding contact angle. A view of the surface with a microscope showed length-wise grooves. Apparently those grooves acted as capillary channels which held water after there was no longer any water flow. This situation should also affect the re-wetting rate since wetting would be a process of water on water-film rather than water on copper. To overcome the above effects, additional polishing was performed with levigated alumina for the copper and stainless steel rods.

In the case of copper, the de-wetting rate was found to decrease slightly with time. This effect was attributed to copper oxidation which

probably has the effect of decreasing the receding contact angle. Rod eccentricity can also affect the values of the wetting and de-wetting flow rates. If the film flow rate is a function of the circumferential position of the rod, the wetting and de-wetting phenomenon will be functions of local flow rates about the circumference rather than the overall flow rate. Thus, an effort was made to maintain symmetry for all the runs.

Table I is a listing of the flow rate data, and the comparison with the analytical equation (19). In the case of copper, only the data at the beginning of a run are listed on table I because of the effects of oxidation on Γ_{d-w} previously mentioned.

Advancing and Receding Contact Angles. - Table II gives the results of the contact angle measurements obtained from the sliding drops. The advancing contact angles are more consistent in their value than the receding contact angles. This could be an indication of a greater sensitivity by the receding angle to surface energy variations.

Comparison with Analysis. - To compare experiment with analysis, the advancing or receding contact angles for a given surface were plotted as a function of the wetting flow rate (fig. 6) and the de-wetting flow rate (fig. 7), respectively. Handbook values of ρ, μ, and γ were used in equation (19). Considering the difficulty in obtaining this type of data and the simplicity of the analysis, the agreement of experiment with analysis is good. This agreement is for wide ranges of the advancing contact angle (37^{o} to 113^{o}) and the receding contact angle (6^{o} to 75^{o}). The results indicated on figs. 6 and 7 point out the importance of specifying whether a surface is being wetted or de-wetted and the value of using the

appropriate dynamic angles on a given surface. Figs. 6 and 7 establish that the greater the contact angle hysteresis, the greater is the ratio of wetting to de-wetting flow rate. In the case of copper this ratio is about 3 to 1.

Direct comparison of the experimental data with the analytical equations is shown in table I. The average percent deviation of experiment from analysis is 30 percent. The greatest deviations occurred for the de-wetting flow rates of copper and stainless steel. This is probably due to the difficulty in accurately measuring the small receding contact angles on copper and stainless steel. Other possible causes of errors are temperature effects and wave motion. Table I shows a fluid temperature range of 12^{o} to 21^{o} C. Ref. 10 suggests a change of contact angle with temperature of $-0.1^{o}/^{o}C$. Considering the experimental variation of the contact angle (table II) and the small effect of temperature on contact angle, the temperature variation is not a significant source of error. As to the effect of waves on the de-wetting rate, this could be important because film breakdown began at the bottom of the rod, where wave motion is fully developed. At the low flow rates, wave effects are probably diminished because of the lowering of the flow rate required to achieve the de-wetting condition. There is a "quieting" of the wave motion with decreased flow rate. The wave effect should become more evident at the higher flow rates such as in the teflon-water case (fig. 7). The de-wetting flow rate for the teflon surface had a greater deviation from the analytical line than the flow rates for the outer surfaces. This could be due to an earlier film breakdown incipience permitted by a thinner than average film

at the valley positions of the waves. The present results did not permit an evaluation of wave effects and in any case if a wave effect does exist it appears to be small.

In these experiments a simple cleaning procedure was used. A check of system cleanliness was made by making surface tension measurements of the water with the ring method before it entered the apparatus and at the exit position. These measurements indicated that the surface energy of the water was unaffected by the test system and that the surface energy was in agreement with accepted values. A factor which can also be important to the value of contact angle is the cleanliness of the surface to be wetted. However, the main objective was to establish the relationship between flow rate and contact angle as given by equation (19). As long as surface conditions remained the same for the measurements of the wetting and de-wetting flow rates and the contact angles, the above objective could be achieved.

Re-examination of Earlier Work

As was mentioned in the literature survey, Hewitt and Lacey (ref. 2) found a lack of agreement with Hartley and Murgatroyd's equation. This work and the work of Ponter et al. (ref. 4) will be re-examined to see if the present modification of Hartley and Murgatroyd's approach, using dynamic contact angles, can explain the apparent discrepancies between various work. In the study of Hewitt and Lacey (ref. 2) the Hartley-Murgatroyd analysis and the static contact angle were used as a means of predicting the film breakdown flow rate. However, the experimental static contact angle of 49^{o} did not give a correct value of the minimum

wetting rate. Instead, to match the minimum wetting rate data a contact angle of 17^{o} was required for use in M-H equation. In ref. 2 the procedure was to unwet an area with a jet of air and then determine if the unwetted area would rewet upon stopping of the air jet. Since the effect of the air jet was to cause a receding interface, it should be expected based on the findings of this paper that the stability of the unwetted area was a function of the receding contact angle. Therefore, in the experiments of ref. 2, use of a contact angle less than the 49^{o} in the analysis of Hartley and Murgatroyd could have been justified. Furthermore, it is likely that with a jet blown at the film, the film is thickened at the periphery of the dry area which tends to rewet the surface when the jet is removed in the manner that wave peaks overrun dry spots (ref. 8). Ponter et al. (ref. 4) studied the system of ethanol-absorption by a falling water film. They reported the flow rates at which natural breakdown of a liquid film occurred. These flow rates for film breakdown could be predicted successfully by equation (1) using their measured contact angles. However, their contact angle measurements were made of water sessile drops in an ethanol-air mixture. The results show an initial decrease in the contact angle before a constant value is reached. This contact angle variation indicates a contact angle hysteresis. A similar trend was observed by the authors in ref. 11 for an evaporating drop. In ref. 11 it was shown that while drop evaporates the contact angle of a sessile drop would decrease from its initial value to the value of the receding contact angle. Therefore, it is possible that when Ponter et al. waited for the contact angle to reduce to a constant value (10 to 40 min),

evaporation could have occurred, resulting in a receding angle rather than a static angle. The receding angle is the contact angle to be used for the analytical prediction of the film breakdown flow rates according to the present work.

Ref. 12 relates the de-wetting of packing material of packed towers to the static contact angle. This approach has much significance in the proper evaluation of the variables governing the wetting flow rates in packed towers. However, since the experiments of ref. 12 determine the conditions when wetted packing material becomes unwetted, the correct contact angle to use is the receding contact angle. An additional piece of information that should be determined for packed towers is the flow rates required for wetting of unwetted packing material as a function of the advancing contact angle. The above information would permit a method of predicting the flow rates required for the wetting of packing material and the permissible decrease in flow rate without causing incomplete wetting or rivulet formation on the packing material.

CONCLUSIONS

1. Whether the initial state of a surface is wetted or unwetted is a determining factor in the flow rate required to form and maintain a continuous liquid film. Forming a moving liquid film on an unwetted surface requires a flow rate which is greater than the flow rate required to maintain a liquid film on a surface.

2. The flow rates required to form a liquid film and to prevent film breakdown may be predicted by a modified version of the Hartley-Murgatroyd analysis (eqs. (18a) and (18b) or eq. (19)). This modified version takes into account the hysteresis of the contact angle associated

with an advancing or receding triple interface.

$$\Gamma^* = 1.69 \left(\frac{\mu\rho}{g}\right)^{1/5} \left[\gamma_{l\text{-}a}(1 - \cos\theta^*)\right]^{3/5} \qquad (19)$$

$\Gamma^* = \Gamma_w$, $\theta^* = \theta_a$ for the case of wetting

$\Gamma^* = \Gamma_{d\text{-}w}$, $\theta^* = \theta_r$ for the case of de-wetting

Film breakdown under adiabatic conditions is governed by the receding contact angle. Formation of a liquid film on an unwetted surface is governed by the advancing contact angle.

REFERENCES

1. Hartley, D. E., and W. Murgatroyd, "Criteria for the Break-up of Thin Liquid Layers Flowing Isothermally Over Solid Surfaces," Int. J. Heat Mass Transfer, 7, 1003 (1964).
2. Hewitt, G. F., and P. M. C. Lacey, "The Breakdown of the Liquid Film in Annular Two-phase Flow," Int. J. Heat Mass Transfer, 8, 781 (1965).
3. Murgatroyd, W., "The Role of Shear and Form Forces in the Stability of a Dry Patch in Two-Phase Film Flow," Int. J. Heat Mass Transfer, 8, 297 (1965).
4. Ponter, A. B., G. A. Davies, and P. G. Thornley, "The Influence of Mass Transfer on Liquid Film Breakdown," Int. J. Heat Mass Transfer, 10, 349 (1967).
5. Zuber, N., and F. W. Staub, "Stability of Dry Patches in Liquid Films Flowing Over Heated Surfaces," Int. J. Heat Mass Transfer, 9, 897 (1966).

6. McPherson, G. D., "Axial Stability of the Dry Patch Formed in Dryout of a Two-Phase Annular Flow," Int. J. Heat Mass Transfer, 13, 1133 (1970).

7. Thompson, T. S., and W. Murgatroyd, "Stability and Breakdown of Liquid Films in Steam Flow with Heat Transfer," Paper B-5 presented at the 4th International Heat Transfer Conference, Versailles, France, 1970.

8. Hsu, Y Y., F. F. Simon, and J. F. Lad, "Destruction of a Thin Liquid Film Flowing Over a Heating Surface," Chem. Engr. Progr. Symp. Ser., 61, (57), 139 (1965).

9. MacDougall, G., and C. Ockrent, "Surface Energy Relations in Liquid/Solid Systems," Proc. Roy. Soc. (London), A180, 151 (194).

10. Ponter, A. B., G. A. Davies, W. Beaton, and T. K. Ross, "The Measurement of Contact Angles Under Conditions of Heat Transfer When a Liquid Film Breaks on a Vertical Surface," Int. J. Heat Mass Transfer, 10, 1633 (1967).

11. Simon, F. F., and Y. Y. Hsu, "Wetting Dynamics of Evaporation Drops on Various Surfaces," NASA TM X-67913 (1971).

12. Ponter, A. B., G. A. Davies, W. Beaton, and T. K. Ross, "Wetting of Packings in Distillation: The Influence of Contact Angle," Trans. Inst. Chem. Engrs., 45, 345 (1967).

Table I. - Experimental Wetting and De-wetting Flow Rates

Surface	t_B, °C	Experimental		Calculated (eq. (19))	
		Γ_w, g/cm-sec	Γ_{d-w}, g/cm-sec	Γ_w, g/cm-sec	Γ_{d-w}, g/cm-sec
Lucite	15		1.08		0.96
	15		1.12		.96
	15	2.38		2.10	
	12		.80		.98
	12	2.16		2.15	
Stainless steel	21		.49		.097
	17	.88		.87	
	20		.33		.098
	21		.32		.097
	15	1.16		.88	
	16	1.12		.88	
	15	1.48		.88	
Teflon	12		2.55		1.96
	12	3.07		2.86	
	12		2.36		1.96
	12	3.01		2.86	
	12	3.18		2.86	
Copper	15	1.71		1.32	
	15		.62		.12
	15	1.79		1.32	
	15		.49		.12

Table II. - Experimental Advancing and Receding Contact Angles

Surface	θ_a, deg	θ_r, deg	$\bar{\theta}_a$, deg	$\bar{\theta}_r$, deg	t_b, °C
Lucite	77	44			22
	82	36			
	83	42			
	85	37			
			82±2	40±3	
Stainless steel	35	6			24
	48	5			
	31	4			
	32	8			
			37±6	6±1	
Teflon	110	75			22
	112	64			
	110	73			
	114	76			
	118	75			
			113±3	75±3	
Copper	44	9			24
	51	7			
	59	7			
	52	4			
	61	--			
			53±5	7±1	

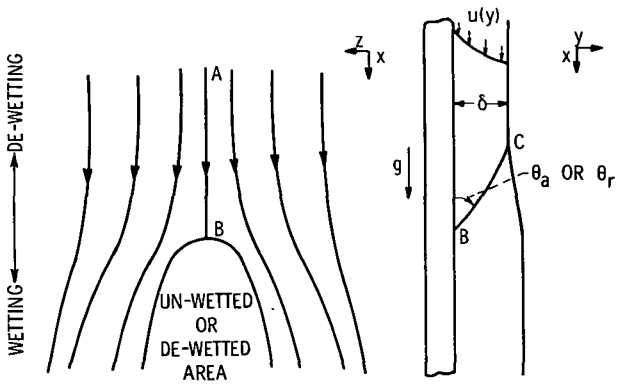

Figure 1. - Wetting and de-wetting film model.

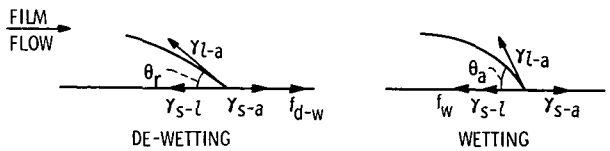

Figure 2. - Vector diagram for receding and advancing contact angles.

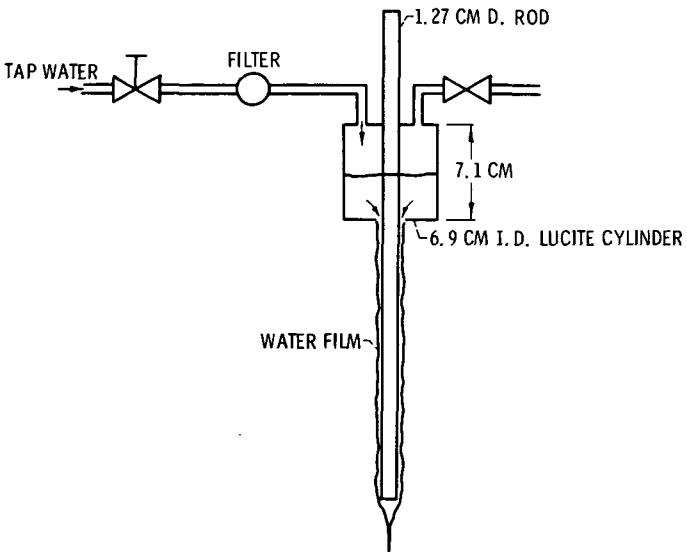

Figure 3. - Experimental apparatus: Wetting and de-wetting flow rate determination.

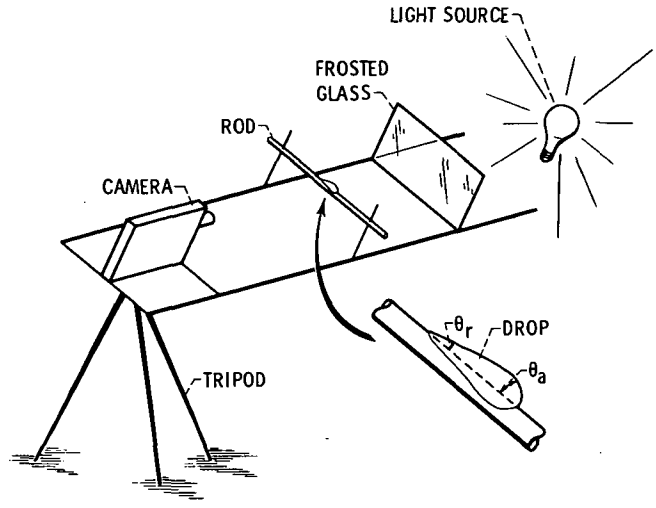

Figure 4. - Experimental apparatus: Advancing and receding contact angles.

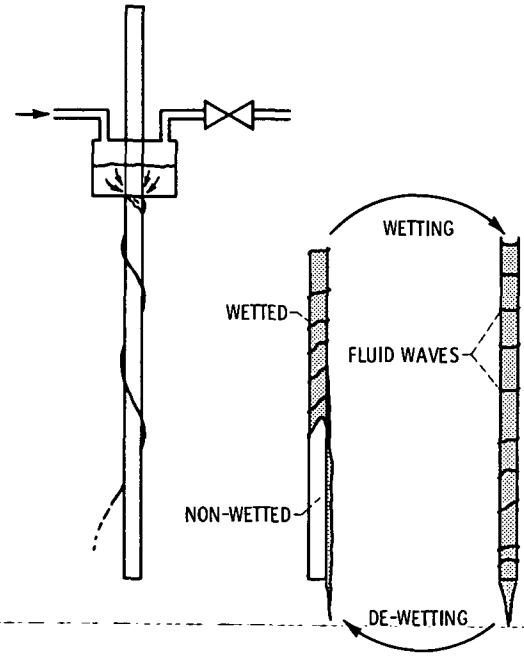

Figure 5. - Observations of film formation and breakdown.

E-6955

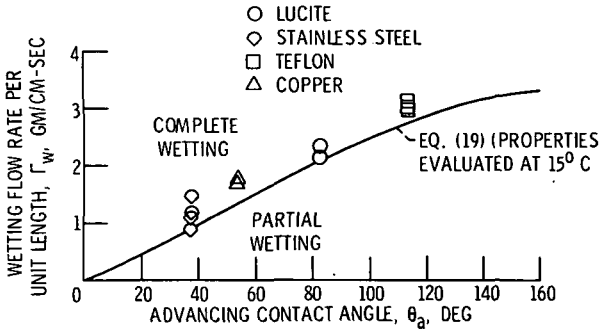

Figure 6. - Flow requirement for wetting by a falling water film as a function of contact angle.

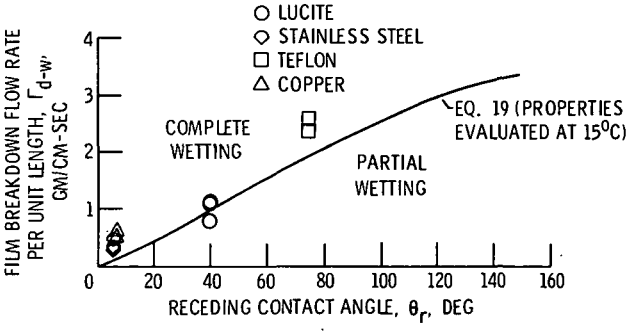

Figure 7. - Falling water film breakdown (de-wetting) flow rate as a function of contact angle.